Proceedings of the Conference
Modern Achievements in Symmetries of Differential Equations
(Symmetry 2022)
Suranaree University of Technology, Thailand
December 13–16, 2022

Rate Type Hypoplastic Differential Equations under Mixed Stress-Strain Control in Biaxial Test

Erich Bauer[1], *Victor A. Kovtunenko*[2,3†], *Pavel Krejčí*[4,5] *and Giselle A. Monteiro*[4]

[1]*Institute of Applied Mechanics, Graz University of Technology, Technikerstr. 4, 8010 Graz, Austria*

[2]*Department of Mathematics and Scientific Computing, University of Graz, NAWI Graz, Heinrichstr.36, 8010 Graz, Austria*

[3]*Lavrent'ev Institute of Hydrodynamics, Siberian Division of the Russian Academy of Sciences, 630090 Novosibirsk, Russia*

[4]*Institute of Mathematics, Czech Academy of Sciences, Žitná 25, 115 67 Praha 1, Czech Republic*

[5]*Faculty of Civil Engineering, Czech Technical University in Prague, Thákurova 7, 166 29 Praha 6, Czech Republic*

Abstract

The hypoplastic constitutive equations stemming from soil mechanics, which are under mixed stress-strain control carried out in a biaxial test, are studied with respect to its well-posedness and non-uniqueness of a solution. The result of theoretical investigation of the strongly nonlinear dynamic system is supported by computer simulation of numerical tests. Besides investigating the existence of global solutions, the simulations give an insight about the numerical convergence and validate the physical consistency of the system of equations when data is chosen in a domain of parameters satisfying feasibility conditions.

Keywords: Hypoplasticity, rate-independent system, implicit differential equation, non-uniqueness.

2020 MSC: Primary 34C55; Secondary 37N15, 74C15, 74L10.

1 Introduction

We study constitutive relations between stress and strain rate describing granular materials, like cohesionless soils or broken rocks, within the hypoplastic theory proposed first by Kolymbas [15], further continued by [26, 27], and extended to barodesy in the recent books [16, 17]. Unlike

†Corresponding author

This work is supported by the OeAD Scientific & Technological Cooperation (WTZ CZ18/2020 and MULT 06/2023) financed by the Austrian Federal Ministry of Science, Research and Economy (BMWFW) and by the Czech Ministry of Education, Youth and Sports (MŠMT), by the GAČR Grant No. 20-14736S, and by the European Regional Development Fund, Project No. CZ.02.1.01/0.0/0.0/16_019/0000778. The Institute of Mathematics of the Czech Academy of Sciences is supported by RVO:67985840.

Email: erich.bauer@tugraz.at (E. Bauer), victor.kovtunenko@uni-graz.at (V. A. Kovtunenko), krejci@math.cas.cz (P. Krejčí), gam@math.cas.cz (G. A. Monteiro)

hyper- and hypoelastic material laws, the hypoplastic response differs for loading and unloading, thus corresponds to inelastic materials. While in classical elastoplastic models the strain is decomposed into elastic and plastic parts, e.g. [1, 8, 14], our approach relies on hypoplastic models of the rate type which are incrementally nonlinear. The interested reader is referred to [25] for a survey on rate-independent processes and hysteresis problems, and to [10–12, 22–24] for an account on mathematical modeling of granular and multiphase media.

Our study considers a simplified version of the hypoplastic constitutive relation that was originally introduced by Bauer [2] and Gudehus [13]. In the previous works [5, 6, 18, 20, 21] we considered the stress-strain rate law as a nonlinear differential equation for the stress under a given proportional strain rate, that we call strain control. Recently, the case of unknown strain rate that should be derived from a given proportional stress, called stress control, was investigated within implicit differential equations in [7, 19]. In the current study, we investigate the case of mixed stress-strain control in a so-called plane strain biaxial test.

In particular, for plane strain conditions we study the response of a hypoplastic material element under constant lateral stress and a monotonic vertical compression/extension. Such tests are of interest in various fields of applied mechanics to study the onset and evolution of shear strain localization [3, 4, 9, 29]. Shear strain localization may occur under a particular stress state where the constitutive equations describe not only continuous homogeneous deformations, but also non-homogeneous deformations. Thus, the system of constitutive equations exhibits non-unique solutions and in the case of a shear band bifurcation two symmetric shear bands may appear. While for the investigation of the onset of strain localization usually the theory of shear-band localization [28] can be applied, the focus of the present paper is based on possible solutions of the system of differential equations under the specified plane strain conditions considered.

2 Plan strain biaxial problem

For coaxial and homogeneous deformation, the tensors of Cauchy stress $\boldsymbol{\sigma}$ and strain rate $\dot{\boldsymbol{\varepsilon}}$ have the diagonal form

$$\boldsymbol{\sigma} = \begin{pmatrix} \sigma_1 & 0 & 0 \\ 0 & \sigma_2 & 0 \\ 0 & 0 & \sigma_3 \end{pmatrix}, \quad \dot{\boldsymbol{\varepsilon}} = \begin{pmatrix} \dot{\varepsilon}_1 & 0 & 0 \\ 0 & \dot{\varepsilon}_2 & 0 \\ 0 & 0 & \dot{\varepsilon}_3 \end{pmatrix}. \tag{2.1}$$

The hypoplastic constitutive equations due to Bauer et al. [6] under the assumption (2.1) are

$$\frac{d\sigma_1}{dt} = f_{\mathrm{s}}\mathrm{tr}\boldsymbol{\sigma}\Big\{a^2\dot{\varepsilon}_1 + \Big(\frac{\boldsymbol{\sigma}:\dot{\boldsymbol{\varepsilon}}}{\mathrm{tr}\boldsymbol{\sigma}}\Big)\frac{\sigma_1}{\mathrm{tr}\boldsymbol{\sigma}} + af_{\mathrm{d}}\Big(\frac{2\sigma_1}{\mathrm{tr}\boldsymbol{\sigma}} - \frac{1}{3}\Big)\|\dot{\boldsymbol{\varepsilon}}\|\Big\}, \tag{2.2}$$

$$\frac{d\sigma_2}{dt} = f_{\mathrm{s}}\mathrm{tr}\boldsymbol{\sigma}\Big\{a^2\dot{\varepsilon}_2 + \Big(\frac{\boldsymbol{\sigma}:\dot{\boldsymbol{\varepsilon}}}{\mathrm{tr}\boldsymbol{\sigma}}\Big)\frac{\sigma_2}{\mathrm{tr}\boldsymbol{\sigma}} + af_{\mathrm{d}}\Big(\frac{2\sigma_2}{\mathrm{tr}\boldsymbol{\sigma}} - \frac{1}{3}\Big)\|\dot{\boldsymbol{\varepsilon}}\|\Big\}, \tag{2.3}$$

$$\frac{d\sigma_3}{dt} = f_{\mathrm{s}}\mathrm{tr}\boldsymbol{\sigma}\Big\{a^2\dot{\varepsilon}_3 + \Big(\frac{\boldsymbol{\sigma}:\dot{\boldsymbol{\varepsilon}}}{\mathrm{tr}\boldsymbol{\sigma}}\Big)\frac{\sigma_3}{\mathrm{tr}\boldsymbol{\sigma}} + af_{\mathrm{d}}\Big(\frac{2\sigma_3}{\mathrm{tr}\boldsymbol{\sigma}} - \frac{1}{3}\Big)\|\dot{\boldsymbol{\varepsilon}}\|\Big\}, \tag{2.4}$$

where the scalar product $\boldsymbol{\sigma}:\dot{\boldsymbol{\varepsilon}} = \sigma_1\dot{\varepsilon}_1+\sigma_2\dot{\varepsilon}_2+\sigma_3\dot{\varepsilon}_3$, and the Frobenius norm $\|\dot{\boldsymbol{\varepsilon}}\| = \sqrt{\dot{\varepsilon}_1^2+\dot{\varepsilon}_2^2+\dot{\varepsilon}_3^2}$. Herein $f_{\mathrm{s}}(t) < 0$ and $f_{\mathrm{d}}(t) > 0$ represent state dependent parameters of the model, and the constant $a > 0$ is related to the yield strength.

In a biaxial test, the following three quantities are prescribed:

$$\dot{\varepsilon}_1 = D_1, \quad \sigma_2 = \sigma_2^0, \quad \dot{\varepsilon}_3 = 0, \tag{2.5}$$

with constant D_1 and $\sigma_2^0 < 0$. In the constitutive relations $\sigma_1(t) < 0$, $\sigma_3(t) < 0$, and $\dot{\varepsilon}_2(t)$ are three unknown functions of time $t \geq 0$. We insert the assumption (2.5) into the hypoplastic

equations such that (2.2)–(2.4) become

$$\frac{d\sigma_1}{dt} = f_s \mathrm{tr}\boldsymbol{\sigma}\Big\{a^2 D_1 + \Big(\frac{\sigma_1 D_1 + \sigma_2^0 \dot\varepsilon_2}{\mathrm{tr}\boldsymbol{\sigma}}\Big)\frac{\sigma_1}{\mathrm{tr}\boldsymbol{\sigma}} + a f_d\Big(\frac{2\sigma_1}{\mathrm{tr}\boldsymbol{\sigma}} - \frac{1}{3}\Big)\sqrt{D_1^2 + \dot\varepsilon_2^2}\Big\}, \tag{2.6}$$

$$0 = f_s \mathrm{tr}\boldsymbol{\sigma}\Big\{a^2 \dot\varepsilon_2 + \Big(\frac{\sigma_1 D_1 + \sigma_2^0 \dot\varepsilon_2}{\mathrm{tr}\boldsymbol{\sigma}}\Big)\frac{\sigma_2^0}{\mathrm{tr}\boldsymbol{\sigma}} + a f_d\Big(\frac{2\sigma_2^0}{\mathrm{tr}\boldsymbol{\sigma}} - \frac{1}{3}\Big)\sqrt{D_1^2 + \dot\varepsilon_2^2}\Big\}, \tag{2.7}$$

$$\frac{d\sigma_3}{dt} = f_s \mathrm{tr}\boldsymbol{\sigma}\Big\{\Big(\frac{\sigma_1 D_1 + \sigma_2^0 \dot\varepsilon_2}{\mathrm{tr}\boldsymbol{\sigma}}\Big)\frac{\sigma_3}{\mathrm{tr}\boldsymbol{\sigma}} + a f_d\Big(\frac{2\sigma_3}{\mathrm{tr}\boldsymbol{\sigma}} - \frac{1}{3}\Big)\sqrt{D_1^2 + \dot\varepsilon_2^2}\Big\}. \tag{2.8}$$

The sum of (2.6)–(2.8) implies the following differential equation for the trace

$$\frac{d(\mathrm{tr}\boldsymbol{\sigma})}{dt} = f_s \mathrm{tr}\boldsymbol{\sigma}\Big\{a^2(D_1 + \dot\varepsilon_2) + \frac{\sigma_1 D_1 + \sigma_2^0 \dot\varepsilon_2}{\mathrm{tr}\boldsymbol{\sigma}} + a f_d\sqrt{D_1^2 + \dot\varepsilon_2^2}\Big\}. \tag{2.9}$$

Denoting for brevity the ratio of the stress tensor scaled with its trace by

$$\hat\sigma_1 = \frac{\sigma_1}{\mathrm{tr}\boldsymbol{\sigma}}, \quad \hat\sigma_2 = \frac{\sigma_2^0}{\mathrm{tr}\boldsymbol{\sigma}}, \quad \hat\sigma_3 = \frac{\sigma_3}{\mathrm{tr}\boldsymbol{\sigma}}, \quad \mathrm{tr}\boldsymbol{\sigma} = \sigma_1 + \sigma_2^0 + \sigma_3, \tag{2.10}$$

we get the following expression for its derivative

$$\frac{d\hat\sigma_n}{dt} = \frac{1}{\mathrm{tr}\boldsymbol{\sigma}}\frac{d\sigma_n}{dt} - \frac{\hat\sigma_n}{\mathrm{tr}\boldsymbol{\sigma}}\frac{d(\mathrm{tr}\boldsymbol{\sigma})}{dt}, \quad n = 1, 3.$$

Hence, from equations (2.9), (2.6) and (2.8) we infer that

$$\frac{d\hat\sigma_1}{dt} = f_s\Big\{a^2 D_1 - a^2(D_1 + \dot\varepsilon_2)\hat\sigma_1 + a f_d\Big(\hat\sigma_1 - \frac{1}{3}\Big)\sqrt{D_1^2 + \dot\varepsilon_2^2}\Big\}, \tag{2.11}$$

$$\frac{d\hat\sigma_3}{dt} = f_s\Big\{-a^2(D_1 + \dot\varepsilon_2)\hat\sigma_3 + a f_d\Big(\hat\sigma_3 - \frac{1}{3}\Big)\sqrt{D_1^2 + \dot\varepsilon_2^2}\Big\}. \tag{2.12}$$

After summation of (2.11) and (2.12), the identity $\hat\sigma_1 + \hat\sigma_2 + \hat\sigma_3 = 1$ leads to

$$\frac{d\hat\sigma_2}{dt} = f_s\Big\{a^2 \dot\varepsilon_2 - a^2(D_1 + \dot\varepsilon_2)\hat\sigma_2 + a f_d\Big(\hat\sigma_2 - \frac{1}{3}\Big)\sqrt{D_1^2 + \dot\varepsilon_2^2}\Big\}. \tag{2.13}$$

Whereas the algebraic equation (2.7) can be rewritten using (2.10) as

$$D_1 \hat\sigma_1 \hat\sigma_2 + (a^2 + \hat\sigma_2^2)\dot\varepsilon_2 + a f_d\Big(2\hat\sigma_2 - \frac{1}{3}\Big)\sqrt{D_1^2 + \dot\varepsilon_2^2} = 0. \tag{2.14}$$

Note that $\hat\sigma_3$ does not enter (2.14), and (2.12) can be deduced from the governing equations. The coupled system (2.11), (2.13), and (2.14) has to be solve with respect to three unknowns $\hat\sigma_1$, $\hat\sigma_2$, and $\dot\varepsilon_2$, endowed with the initial conditions:

$$\hat\sigma_1(0) = \frac{\sigma_1^0}{\sigma_1^0 + \sigma_2^0 + \sigma_3^0}, \quad \hat\sigma_2(0) = \frac{\sigma_2^0}{\sigma_1^0 + \sigma_2^0 + \sigma_3^0}, \tag{2.15}$$

for prescribed $\sigma_1^0 < 0$, $\sigma_3^0 < 0$, and σ_2^0 from (2.5).

Theorem 2.1 (Solution)**.** *A solution to the linear Cauchy system* (2.11) *and* (2.13) *under initial conditions* (2.15) *and constrained by* (2.14) *can be written in the integral form:*

$$\hat\sigma_1(t) - \frac{1}{3} = e^{\int_0^t \phi_3(\tau)\,d\tau}\Big[\hat\sigma_1(0) - \frac{1}{3} + \int_0^t \phi_1(\xi) e^{-\int_0^\xi \phi_3(\tau)\,d\tau} d\xi\Big], \tag{2.16}$$

$$\hat\sigma_2(t) - \frac{1}{3} = e^{\int_0^t \phi_3(\tau)\,d\tau}\Big[\hat\sigma_2(0) - \frac{1}{3} + \int_0^t \phi_2(\xi) e^{-\int_0^\xi \phi_3(\tau)\,d\tau} d\xi\Big], \tag{2.17}$$

where the integrands are

$$\phi_1 = a^2 f_s \frac{2D_1 - \dot\varepsilon_2}{3}, \quad \phi_2 = a^2 f_s \frac{2\dot\varepsilon_2 - D_1}{3}, \quad \phi_3 = a^2 f_s \Big\{ -(D_1 + \dot\varepsilon_2) + \frac{f_d}{a}\sqrt{D_1^2 + \dot\varepsilon_2^2} \Big\}. \tag{2.18}$$

Moreover, under the solvability condition

$$\mathcal{D} := a^2 f_d^2 D_1^2 \Big(2\hat\sigma_2 - \frac{1}{3}\Big)^2 \Big\{ \hat\sigma_1^2 \hat\sigma_2^2 + \big(a^2 + \hat\sigma_2^2\big)^2 - a^2 f_d^2 \Big(2\hat\sigma_2 - \frac{1}{3}\Big)^2 \Big\} \geq 0 \tag{2.19}$$

(where the discriminant $\mathcal{D}$ becomes zero for $\hat\sigma_2 = 1/6$), from the algebraic equation (2.14) we deduce two possible expressions for $\dot\varepsilon_2$, namely

$$(\dot\varepsilon_2)_\pm = \frac{D_1 \hat\sigma_1 \hat\sigma_2 (a^2 + \hat\sigma_2^2) \pm \sqrt{\mathcal{D}}}{a^2 f_d^2 \big(2\hat\sigma_2 - \frac{1}{3}\big)^2 - \big(a^2 + \hat\sigma_2^2\big)^2}. \tag{2.20}$$

Proof. Using the notation (2.18) we can rewrite (2.11) and (2.13) in a unified way as

$$\frac{d}{dt}\Big(\hat\sigma_n - \frac{1}{3}\Big) = \phi_n + \phi_3 \Big(\hat\sigma_n - \frac{1}{3}\Big), \quad n = 1, 2. \tag{2.21}$$

The multiplication of (2.21) by the factor $\exp(-\int_0^t \phi_3(\tau)\,d\tau)$ yields the equivalent equation

$$\frac{d}{dt}\Big[\Big(\hat\sigma_n(t) - \frac{1}{3}\Big) e^{-\int\limits_0^t \phi_3(\tau)\,d\tau}\Big] = \phi_n(t) e^{-\int\limits_0^t \phi_3(\tau)\,d\tau}, \quad n = 1, 2.$$

Thus, formulas (2.16) and (2.17) can be obtained by simple integration over the interval $[0, t]$ and taking into account the initial values given in (2.15).

Considering the aforementioned $\hat\sigma_1$ and $\hat\sigma_2$, from (2.14) we deduce a quadratic equation for the unknown $\dot\varepsilon_2$ as follows:

$$\Big[a^2 f_d^2 \Big(2\hat\sigma_2 - \frac{1}{3}\Big)^2 - \big(a^2 + \hat\sigma_2^2\big)^2\Big]\dot\varepsilon_2^2 - 2D_1 \hat\sigma_1 \hat\sigma_2 (a^2 + \hat\sigma_2^2)\dot\varepsilon_2 + D_1^2 \Big[a^2 f_d^2 \Big(2\hat\sigma_2 - \frac{1}{3}\Big)^2 - \hat\sigma_1^2 \hat\sigma_2^2\Big] = 0, \tag{2.22}$$

whose discriminant $\mathcal{D}$ is given in (2.19), and consequently we have two possible solutions $(\dot\varepsilon_2)_\pm$ as in (2.20). Note that (2.19) ensures that $\mathcal{D}$ is non-negative independently of the sign of D_1. The proof is completed. □

For a physically consistent model relevant for cohesionless granular materials, only negative normal stresses are admissible. Therefore, $\mathrm{tr}\boldsymbol{\sigma} < 0$, and formula (2.10) leads to the restriction $\hat\sigma_n = \sigma_n / \mathrm{tr}\boldsymbol{\sigma} > 0$ for $n = 1, 2, 3$.

3 Numerical simulations

Based on Theorem 2.1, we analyze the existence of numerical solutions for two systems with unknowns $\hat\sigma_1$, $\hat\sigma_2$, and $\dot\varepsilon_2$ and accounting for the plain strain biaxial model in the form of Cauchy problem (2.11), (2.13)–(2.15). Note that the normalized stresses $\hat\sigma_1, \hat\sigma_2 \in (0, 1)$ as unknown variables in the linear equations (2.11), (2.13) are numerically advantageous over the stresses σ_1, σ_3 in the nonlinear equations (2.6), (2.8), which are unbounded in general. After finding the solution, we can determine the quantities $\hat\sigma_3$ and $\mathrm{tr}\boldsymbol{\sigma}$ in (2.9) and (2.12) which are implicitly given by

$$\hat\sigma_3 = 1 - \hat\sigma_1 - \hat\sigma_2, \quad \mathrm{tr}\boldsymbol{\sigma} = \frac{\sigma_2^0}{\hat\sigma_2}. \tag{3.1}$$

To make our presentation of the numerical scheme more precise, we distinguish the two systems comprehending equations (2.11), (2.13), and (2.20) taking into account the discriminant as in (2.19), which are gathered as follows:

$$\begin{aligned}
\mathcal{D} &= a^2 f_{\mathrm{d}}^2 D_1^2 \Big(2\hat{\sigma}_2 - \frac{1}{3}\Big)^2 \Big\{\hat{\sigma}_1^2\hat{\sigma}_2^2 + \big(a^2 + \hat{\sigma}_2^2\big)^2 - a^2 f_{\mathrm{d}}^2 \Big(2\hat{\sigma}_2 - \frac{1}{3}\Big)^2\Big\},\\
\dot{\varepsilon}_2 &= \frac{D_1\hat{\sigma}_1\hat{\sigma}_2(a^2 + \hat{\sigma}_2^2) - \sqrt{\mathcal{D}}}{a^2 f_{\mathrm{d}}^2\big(2\hat{\sigma}_2 - \frac{1}{3}\big)^2 - \big(a^2 + \hat{\sigma}_2^2\big)^2},\\
\frac{d\hat{\sigma}_1}{dt} &= f_{\mathrm{s}}\Big\{a^2 D_1 - a^2(D_1 + \dot{\varepsilon}_2)\hat{\sigma}_1 + a f_{\mathrm{d}}\Big(\hat{\sigma}_1 - \frac{1}{3}\Big)\sqrt{D_1^2 + \dot{\varepsilon}_2^2}\Big\},\\
\frac{d\hat{\sigma}_2}{dt} &= f_{\mathrm{s}}\Big\{a^2\dot{\varepsilon}_2 - a^2(D_1 + \dot{\varepsilon}_2)\hat{\sigma}_2 + a f_{\mathrm{d}}\Big(\hat{\sigma}_2 - \frac{1}{3}\Big)\sqrt{D_1^2 + \dot{\varepsilon}_2^2}\Big\},
\end{aligned} \tag{$-\sqrt{\mathrm{D}}$}$$

and

$$\begin{aligned}
\mathcal{D} &= a^2 f_{\mathrm{d}}^2 D_1^2 \Big(2\hat{\sigma}_2 - \frac{1}{3}\Big)^2 \Big\{\hat{\sigma}_1^2\hat{\sigma}_2^2 + \big(a^2 + \hat{\sigma}_2^2\big)^2 - a^2 f_{\mathrm{d}}^2 \Big(2\hat{\sigma}_2 - \frac{1}{3}\Big)^2\Big\},\\
\dot{\varepsilon}_2 &= \frac{D_1\hat{\sigma}_1\hat{\sigma}_2(a^2 + \hat{\sigma}_2^2) + \sqrt{\mathcal{D}}}{a^2 f_{\mathrm{d}}^2\big(2\hat{\sigma}_2 - \frac{1}{3}\big)^2 - \big(a^2 + \hat{\sigma}_2^2\big)^2},\\
\frac{d\hat{\sigma}_1}{dt} &= f_{\mathrm{s}}\Big\{a^2 D_1 - a^2(D_1 + \dot{\varepsilon}_2)\hat{\sigma}_1 + a f_{\mathrm{d}}\Big(\hat{\sigma}_1 - \frac{1}{3}\Big)\sqrt{D_1^2 + \dot{\varepsilon}_2^2}\Big\},\\
\frac{d\hat{\sigma}_2}{dt} &= f_{\mathrm{s}}\Big\{a^2\dot{\varepsilon}_2 - a^2(D_1 + \dot{\varepsilon}_2)\hat{\sigma}_2 + a f_{\mathrm{d}}\Big(\hat{\sigma}_2 - \frac{1}{3}\Big)\sqrt{D_1^2 + \dot{\varepsilon}_2^2}\Big\}.
\end{aligned} \tag{$+\sqrt{\mathrm{D}}$}$$

In both cases we consider the initial conditions in (2.15) with the constant parameters yet to be prescribed.

The local solutions to ($-\sqrt{\mathrm{D}}$) and ($+\sqrt{\mathrm{D}}$) might be ensured for $t \in [0, t_0]$ with small $t_0 > 0$. However, our interest concerns global solutions for arbitrary $t \geq 0$, and, if a global solution to either ($-\sqrt{\mathrm{D}}$) or ($+\sqrt{\mathrm{D}}$) exists, in its asymptotic behavior for growing t.

To measure an error of numerical schemes applied, we suggest to estimate the residual of the algebraic equation (2.7):

$$\mathrm{Res} := f_{\mathrm{s}}\mathrm{tr}\boldsymbol{\sigma}\Big\{a^2\dot{\varepsilon}_2 + \Big(\frac{\sigma_1 D_1 + \sigma_2^0\dot{\varepsilon}_2}{\mathrm{tr}\boldsymbol{\sigma}}\Big)\frac{\sigma_2^0}{\mathrm{tr}\boldsymbol{\sigma}} + a f_{\mathrm{d}}\Big(\frac{2\sigma_2^0}{\mathrm{tr}\boldsymbol{\sigma}} - \frac{1}{3}\Big)\sqrt{D_1^2 + \dot{\varepsilon}_2^2}\Big\}. \tag{3.2}$$

From our numerical tests we can report the following features. Refining the uniform time mesh, numerical iterations may diverge or leave a region of the physical consistency, the residual error may remain large or converge very slow, thus theoretical solution be numerically unattainable. Typically we observe only one numerically reasonable and physically consistent solution.

3.1 Biaxial extension test

For a first simulation test, we prescribe the initial stresses and the constant strain rate $\dot{\varepsilon}_1$ to be

$$\sigma_1^0 = \sigma_2^0 = \sigma_3^0 = -100, \quad \text{and} \quad D_1 = 1, \tag{3.3}$$

which implies an isotropic state in a domain of parameters satisfying the feasibility conditions. In view of (2.5) and taking into account the sign convention of rational mechanics, the choice $D_1 = 1$ describes a state of vertical extension with a constant strain rate 1. The material parameters for the hypoplastic equations (2.2)–(2.4) are taken from [18]:

$$a = 0.33, \quad f_{\mathrm{d}} = 1, \quad f_{\mathrm{s}} = -550.$$

These data satisfy the solvability condition (2.19) at $t = 0$ and, by continuity, the condition also holds true, at least, in an interval $[0, t_0]$, with some $t_0 > 0$.

Since the constitutive equations are rate independent, we opted for the representation of numerical results with respect to the vertical strain rather than the time evolution. The numerical result for solution $(\sigma_1(t), \varepsilon_2(t), \sigma_3(t))$ of $(+\sqrt{\mathrm{D}})$ under data set (3.3) and a constant lateral stress σ_2 obtained with a MAPLE code is depicted versus the vertical strain $\varepsilon_1(t) = D_1 t$ from (2.5) for $t \in (0, 0.04)$ in the four plots of Figure 1.

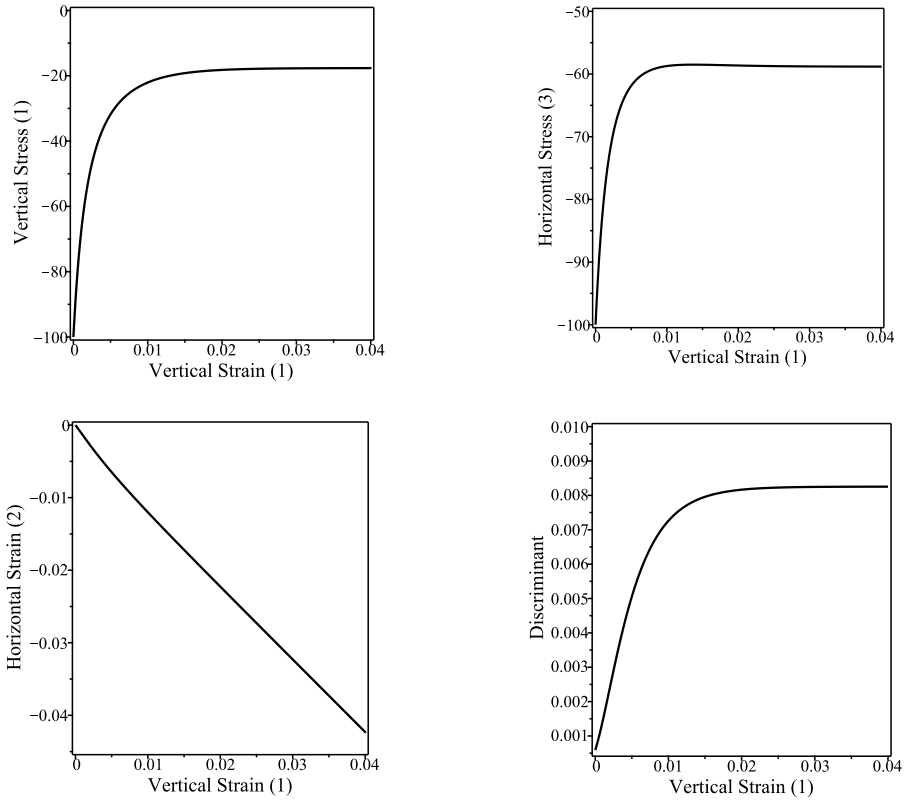

Figure 1: The simulation test of biaxial extension under data set (3.3).

In the upper left and right plots of Figure 1 the first (vertical) and the third (horizontal) stress components are depicted. We observe that the evolution is physically consistent: $\sigma_1 < 0$ and $\sigma_3 < 0$ stress components remain negative during extension and tend from below towards asymptotic values which are related to the parameter a for the stress limit state. In the lower left plot of Figure 1, the horizontal strain component $\varepsilon_2(t)$ is calculated from its rate $\dot{\varepsilon}_2(t)$ and the initial value $\varepsilon_2(0) = 0$. We remark that the strain $\varepsilon_2 \leq 0$ in this case, that is, when extension takes place. Evolution of the discriminant $\mathcal{D}$ is presented in the lower right plot of Figure 1. We can observe that the discriminant is strictly positive and tends towards an asymptotic value.

To check if the solutions converge or diverge by the time discretization, the system of differential algebraic equation is solved in MATLAB using the standard solver RK4. In Figure 2 we show in the log-log scale the absolute value of the residual for the numerical solution of the system $(+\sqrt{\mathrm{D}})$ when decreasing the time mesh size as $\{10^{-5}, 10^{-4}, 10^{-3}, 10^{-2}\}$. For this we calculate the average of |Res| in (3.2) over time for the current states under equdistant meshing by 101, 1001, 10001, 100001 time points, respectively. In Figure 2 a high rate of convergence of the solution $(+\sqrt{\mathrm{D}})$ when refining the mesh is clearly observed. The evolution of the system $(-\sqrt{\mathrm{D}})$ is not presented here, since its residual is large of order 10^4 and converges very slowly such that the limit (if exists) is numerically unattainable.

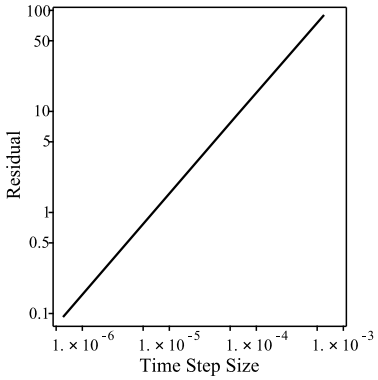

Figure 2: Log-log plot of the residual for $(+\sqrt{\mathrm{D}})$ versus time step size.

3.2 Biaxial compression test

Now let us consider the initial values as defined above but changing the sign of the strain rate, that is,

$$\sigma_1^0 = \sigma_2^0 = \sigma_3^0 = -100, \quad \text{and} \quad D_1 = -1, \tag{3.4}$$

which describes a state of vertical compression with a constant strain rate -1.

In this test, the standard numerical schemes are not well behaved. Therefore, from the two possible solutions $\dot{\varepsilon}_2$ we select the one which minimizes the value of |Res| in (3.2). The general idea of the such selection procedure is commonly used in many numerical methods in which the solution is based on the minimum of a defined residual. Indeed, if we look at the evolution of the residual Res calculated from $(+\sqrt{\mathrm{D}})$ and $(-\sqrt{\mathrm{D}})$ as drawn in the left and right plots of Figure 3, respectively, we observe a point approximately $\varepsilon_1 = -0.01324$, where the zero residual switches from $(+\sqrt{\mathrm{D}})$ to $(-\sqrt{\mathrm{D}})$.

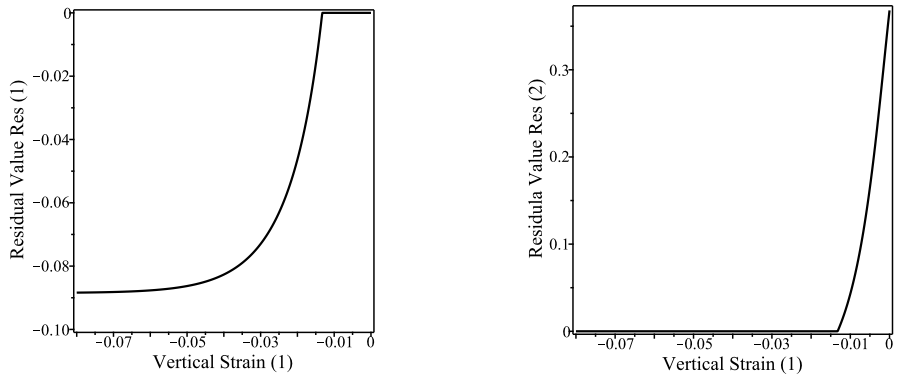

Figure 3: The residual Res in (3.2) for $(+\sqrt{\mathrm{D}})$ and $(-\sqrt{\mathrm{D}})$.

The corresponding numerical solution is depicted versus the vertical strain $\varepsilon_1 = D_1 t$ for $t \in (0, 0.08)$ in Figure 4. We can see in the upper left and right plots that $\sigma_1 < 0$ and $\sigma_3 < 0$. Under the axial compression, the amount of both the vertical stress and the horizontal stress increases, which is physically consistent. Moreover, the stress components show an asymptotical behaviour with continued vertical compression. Note that in the lower left plot $\varepsilon_2 \geq 0$ during the whole evolution. In contrast to the extension test, in the lower right plot the discriminant $\mathcal{D}$ decreases at the beginning of vertical compression, becomes zero at the vertical strain of approximately $\varepsilon_1 = -0.01324$, and afterwards it slightly increases and reaches an almost constant value. Exactly this state is relevant to switch for the solution of $\dot{\varepsilon}_2$ from $(+\sqrt{\mathrm{D}})$ to $(-\sqrt{\mathrm{D}})$.

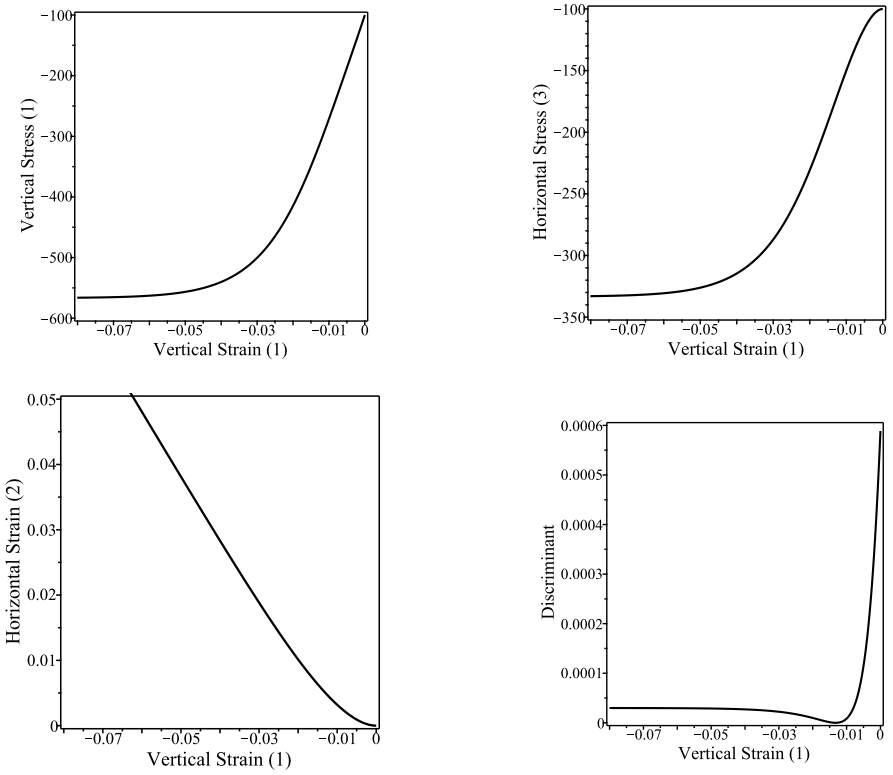

Figure 4: The simulation test of biaxial compression under data set (3.4).

4 Conclusion

We have studied well-posedness of the hypoplastic constitutive equations carried out in a plane strain biaxial test. Under mixed stress-strain control, we construct two systems of differential algebraic equations, corresponding to the strain rate obtained by solving a quadratic equation. In numerical simulations we find a single feasible solution, provided that the data are chosen in a domain of parameters satisfying the proposed solvability conditions. More detailed investigations are still under way and the results are the topic of an future publication.

References

[1] B. D. Annin, V. A. Kovtunenko and V. M. Sadovskii, *Variational and hemivariational inequalities in mechanics of elastoplastic, granular media, and quasibrittle cracks*, in: "Analysis, Modelling, Optimization, and Numerical Techniques", G. O. Tost and O. Vasilieva, editors, pp. 49–56, Springer Proc. Math. Stat. **121**, 2015.

[2] E. Bauer, *Calibration of a comprehensive hypoplastic model for granular materials*, Soils Found. **36** (1996), 13–26.

[3] E. Bauer, *Analysis of shear band bifurcation with a hypoplastic model for a pressure and density sensitive granular material*, Mech. Mater. **31** (1999), 597–609.

[4] E. Bauer and W. Huang, *Influence of density and pressure on spontaneous shear band formations in granular materials*, in: "IUTAM Symposium on Theoretical and Numerical Methods in Continuum Mechanics of Porous Materials", W. Ehlers, editor, Solid Mechanics and Its Applications **87**, pp. 245–25, Springer, Dordrecht, 2001.

[5] E. Bauer, V. A. Kovtunenko, P. Krejčí, N. Krenn, L. Sováková and A. V. Zubkova, *Modified model for proportional loading and unloading of hypoplastic materials*, in: "Extended Abstracts Spring 2018. Singularly Perturbed Systems, Multiscale Phenomena and Hysteresis: Theory and Applications", A. Korobeinikov, M. Caubergh, T. Lázaro and J. Sardanyés, editors, Trends in Mathematics **11**, pp. 201–210, Birkhäuser, Ham, 2019.

[6] E. Bauer, V. A. Kovtunenko, P. Krejčí, N. Krenn, L. Sováková and A. V. Zubkova, *On proportional deformation paths in hypoplasticity*, Acta Mechanica **231** (2020), 1603–1619.

[7] E. Bauer, V. A. Kovtunenko, P. Krejčí, G. A. Monteiro and J. Runcziková, *Stress-controlled ratchetting in hypoplasticity*, Acta Mechanica **234** (2023), 4077–4093.

[8] M. Brokate and P. Krejčí, *Wellposedness of kinematic hardening models in elastoplasticity*, RAIRO Modél. Math. Anal. Numér. **32** (1998), 177–209.

[9] R. Chambon, J. Desrues and D. Tillard, *Shear moduli identification versus experimental localization data*, in: "Proceedings of the 3rd International Workshop on Localization and Bifurcation Theory of Soils and Rock", pp. 101–111, A.A.Belkema, Rotterdam, 1994.

[10] K. Fellner and V. A. Kovtunenko, *A singularly perturbed nonlinear Poisson–Boltzmann equation: uniform and super-asymptotic expansions*, Math. Meth. Appl. Sci. **38** (2015), 3575–3586.

[11] K. Fellner and V. A. Kovtunenko, *A discontinuous Poisson–Boltzmann equation with interfacial transfer: homogenisation and residual error estimate*, Appl Anal. **95** (2016), 2661–2682.

[12] J. R. González Granada and V. A. Kovtunenko, *Entropy method for generalized Poisson–Nernst–Planck equations*, Anal. Math. Phys. **8** (2018), 603–619.

[13] G. Gudehus, *A comprehensive constitutive equation for granular materials*, Soils Found. **36** (1996), 1–12.

[14] A. M. Khludnev and V. A. Kovtunenko, *Analysis of Cracks in Solids*, WIT-Press, Southampton, Boston, 2000.

[15] D. Kolymbas, *Introduction to Hypoplasticity*, A.A. Balkema, Rotterdam, 2000.

[16] D. Kolymbas, *A Primer on Theoretical Soil Mechanics*, Cambridge Univ. Press, 2022.

[17] D. Kolymbas and G. Medicus, *Genealogy of hypoplasticity and barodesy*, Int. J. Numer. Anal. Methods Geomech. **40** (2016), 2532–2550.

[18] V. A. Kovtunenko, E. Bauer, J. Eliaš, P. Krejčí, G. A. Monteiro and L. Straková (Sováková), *Cyclic behavior of simple models in hypoplasticity and plasticity with nonlinear kinematic hardening*, J. Sib. Fed. Univ. - Math. Phys. **14** (2021), 756–767.

[19] V. A. Kovtunenko, J. Eliaš, P. Krejčí, G. A. Monteiro and J. Runcziková, *Stress-controlled hysteresis and long-time dynamics of implicit differential equations arising in hypoplasticity*, Arch. Math. (Brno), **59** (2023), 275-286.

[20] V. A. Kovtunenko, P. Krejčí, E. Bauer, L. Sováková and A. V. Zubkova, *On Lyapunov stability in hypoplasticity*, in: "Proc. Equadiff 2017 Conference", K. Mikula, D. Ševčovič and J. Urbán, editors, pp. 107–116, Slovak University of Technology, Bratislava, 2017.

[21] V. A. Kovtunenko, P. Krejčí, N. Krenn, E. Bauer, L. Sováková and A. V. Zubkova, *On feasibility of rate-independent stress paths under proportional deformations within hypoplastic constitutive model for granular materials*, Mathematical Models in Engineering **5** (2019), 119–126.

[22] V. A. Kovtunenko and A. V. Zubkova, *Mathematical modeling of a discontinuous solution of the generalized Poisson–Nernst–Planck problem in a two-phase medium*, Kinet. Relat. Mod. **11** (2018), 119–135.

[23] V. A. Kovtunenko and A. V. Zubkova, *Homogenization of the generalized Poisson–Nernst–Planck problem in a two-phase medium: correctors and estimates*, Appl Anal. **100** (2021a), 253–274.

[24] V. A. Kovtunenko and A. V. Zubkova, *Existence and two-scale convergence of the generalised Poisson–Nernst–Planck problem with non-linear interface conditions*, Eur. J. Appl. Math. **32** (2021b), 683–710.

[25] P. Krejčí, *Hysteresis, Convexity and Dissipation in Hyperbolic Equations*, Gakkotosho, Tokyo, 1996.

[26] D. Mašín, *Modelling of Soil Behaviour with Hypoplasticity: Another Approach to Soil Constitutive Modelling*, Springer Nature, Switzerland, 2019.

[27] A. Niemunis and I. Herle, *Hypoplastic model for cohesionless soils with elastic strain range*, Mech. Cohes.-Frict. Mat. **2** (1997), 279–299.

[28] J. Rudnicki and J. Rice, *Conditions for the localization of deformation in pressure sensitive dilatant materials*, J. Mech. Phys. Solids **23** (1975), 371–394.

[29] I. Vardoulakis, *Shear band inclination and shear modulus of sand in biaxial tests*, Int. J. Numer. Anal. Meth. Geomech. **4** (1980), 103–119.